Biochimica et Biophysica Acta, 1152 (1993) 135–145

BBAMEM 76100

Phase equilibria and local structure in binary lipid bilayers

Kent Jørgensen [a], Maria M. Sperotto [b], Ole G. Mouritsen [b,c,*], John Hjort Ipsen [b] and Martin J. Zuckermann [d]

[a] *Department of Pharmacology, University of Virginia, Charlottesville, VA 22908 (USA),* [b] *Department of Physical Chemistry, The Technical University of Denmark, Building 206, DK-2800 Lyngby (Denmark),* [c] *Canadian Institute of Advanced Research, Vancouver, B.C. (Canada) and* [d] *Centre for the Physics of Materials, Department of Physics, McGill University, Montréal, Québec (Canada)*

(Received 8 March 1993)
(Revised manuscript received 24 June 1993)

Key words: Binary lipid bilayer; Phase diagram; Specific heat; Local structure; Correlation function

A molecular interaction model is used to describe the phase diagram of two-component phospholipid bilayer membranes of saturated phospholipids, DC_nPC, with different acyl-chain lengths, $n = 12,14,18,20$. The interaction between acyl chains of different length is formulated in terms of a hydrophobic mismatch which permits the series of binary phase diagrams to be calculated in terms of a single 'universal' interaction parameter. The properties of the model are calculated by computer-simulation techniques which not only permit determination of the specific-heat function and the phase diagram but also reveal the local structure of the mixture in the different parts of the phase diagram. The local structure is described pictorially and characterized quantitatively in terms of a correlation function. It is shown that the non-ideal mixing of lipid species due to mismatch in the hydrophobic lengths leads to a progressively increasing local ordering as the chain-length difference is increased. A pronounced local structure is found to persist deep inside the fluid phase of the mixture. The local structure is discussed in relation to the features observed in the specific-heat function, for which theoretical data, as well as experimental data obtained from differential-scanning calorimetry are presented.

I. Introduction

One-component lipid bilayers exhibit a series of themotropic phase transitions [1] which are of relevance to biological membranes [2,3]. One of these transitions is the gel-fluid phase transition. Natural membranes are not one-component systems but contain a large number of different lipid species in addition to proteins. Such multi-component systems have complex phase diagrams with regions of thermodynamic coexistence. In an attempt to understand the phase equilibria in the multi-component systems basically two major types of simple few-component model membrane systems are commonly studied: (i) one-component lipid bilayers incorporated with polypeptides, proteins, sterols, etc., and (ii) two- or more component lipid mixtures.

It is still a controversial issue as to whether phase transitions and phase equilibria in lipid membranes have any direct influence on the functioning of membranes [1,2,4,5]. Non-lamellar membrane phases, such as hexagonal and cubic phases, have been suggested as important for a variety of membrane functions [6]. In relation to the gel-fluid phase transition in lamellar bilayer phases, the most common counter argument to attaching significance to membrane phase equilibria in a functional context is that most membrane systems are thought to be in a type of 'fluid' phase under physiological conditions. Furthermore, it is often tacitly assumed, as inferred by cartoons for the classic fluid-mosaic membrane model, that a fluid membrane phase may be thought of as a random liquid mixture with no appreciable degree of local ordering or structure. This assumption is not generally fulfilled, since it is well-known that the nature of this fluid phase reflects the underlying phase equilibria and phase diagram of the membrane considered as a multi-component mixture. In fact multi-component systems support cooperative phenomena which determine not only the phase diagram but also the local and the global structure of the different phases, in particular the fluid phase.

* Corresponding author. Fax: +45 45 934808.
Abbreviations: DC_nPC, saturated di-acyl phospatidylcholine with n carbon atoms in the acyl chain

Recently, a series of model membrane studies have been published about the nano-scale structure and connectivity of coexisting domains in the gel-fluid coexistence regions of binary lipid mixtures, such as $DC_{14}PC$–$DC_{18}PC$ [7–11]. It has been convincingly demonstrated by fluorescence recovery and EPR probe measurements that such domains exist and that their percolation properties are important for in-plane bimolecular reactions in membranes [12]. It is likely that coexistence of gel and fluid lipid domains is relevant for function in some types of biological membranes [13]. None of these experimental studies, which were applied to the gel-fluid coexistence region, have as yet been extended to study local structure in the fluid phase possibly because of the inherent difficulty of distinguishing between different types of fluid lipid domains.

In this paper we provide evidence, based on a theoretical model study, that the underlying phase equilibria of binary lipid mixtures lead to pronounced local ordering in the fluid phase. This type of lipid microstructure is more subtle and extends over smaller length scales than those characterizing the lipid domains in the gel-fluid coexistence region. The local ordering in the fluid phase is dynamically maintained by fluctuations and leads to dynamic membrane heterogeneity which may well be of importance for membrane function [14,15]. In this case the local structure is described in terms of compositional fluctuations indicating that the local concentration of a given lipid species may be different from the global (average) concentration. The typical spatial correlation length (ξ) of the local ordering depends on the thermodynamic conditions, specifically the temperature and the composition, as well as the distance from certain features in the phase diagram. The local ordering is more pronounced the more non-ideal the mixture becomes. In the present work we have studied these conditions by considering a class of binary lipid mixtures where the degree of non-ideality can be varied in a simple way. Specifically we have studied two-component phospholipid bilayer membranes of saturated phospholipids, DC_nPC, with different acyl-chain lengths, n = 12,14,18,20. The larger the difference in acyl-chain length becomes, the more non-ideal the mixture behaves [16]. Typical values of the correlation length (ξ) for these mixtures are in the range $\xi \leqq 5$–50 Å but ξ becomes much higher near special points in the phase diagram (critical mixing points or incipient critical points).

Local ordering on the scale of less than 50 Å is difficult to detect directly in conventional experiments (such as optical spectroscopy), whereas compositional fluctuations on length scales larger than approx. 100 Å can be detected by small-angle neutron scattering [17,18]. The fluctuations in local ordering may be detected indirectly via their manifestation in bulk membrane properties, such as the specific heat [20] which, however, is most sensitive to fluctuations involving both fluid and gel lipid domains. In the present work we took a two-faceted approach to the problem of membrane fluctuations and local ordering. First we used a molecular interaction model for binary lipid mixtures together with computer-simulation techniques which allow not only global thermodynamic properties to be determined, such as specific heat and phase diagram, but also permit direct inspection of the lateral organization of the bilayer mixture. Secondly, we performed differential-scanning calorimetry experiments across the gel-fluid coexistence region of the $DC_{14}PC$–$DC_{18}PC$ binary mixture and studied the wings of the specific heat function which reflects the membrane fluctuations. This mixture has previously been investigated by differential-scanning calorimetry, e.g., in the early work by Mabrey and Sturtevant [19]. The molecular model is described in Section II and the experimental procedures are given in Section III. The results of computer simulations for the lipid mixtures are reported in Section IV and a comparison with our experimental results is presented in Section V. Section VI contains a discussion of future work, together with a statement about the effect of drug and anesthetic molecules on the phase behavior of the lipid mixtures.

II. Microscopic model and calculational techniques

Microscopic model

The microscopic molecular interaction model used in the present paper for binary lipid mixtures builds on the 10-state Pink model [21] to describe the gel-fluid transition for each of the pure lipid-bilayer components of the mixture in the fully hydrated state. The two lipid species are coupled by a term which reflects the incompatibility of acyl chains of different hydrophobic lengths. This type of hydrophobic mismatch interaction, which is related to the mismatch interaction of the so-called mattress model of lipid-protein interactions [22–24], was recently used in a study of lipid selectivity of integral proteins embedded in binary lipid mixtures (Sperotto, M.M. and Mouritsen, O.G., unpublished data). Since the 10-state Pink model has been described in detail in several previous publications [21,25], a short description of the model will be sufficient here.

The Hamiltonian function for the binary mixture of the two lipid species A and B is written

$$\mathscr{H} = \mathscr{H}^{A} + \mathscr{H}^{B} + \mathscr{H}^{AB} \tag{1}$$

where the two first terms describe the interaction between alike species and the last term the interaction

between different species. The 10-state Pink model for species A (and similarly for species B) reads

$$\mathcal{H}^{A} = \sum_{i}\sum_{\alpha}\left(E_{\alpha}^{A} + \Pi A_{\alpha}^{A}\right)\mathcal{L}_{i\alpha}^{A} - \frac{J_A}{2}\sum_{i,j}\sum_{\alpha,\beta} I_{\alpha}^{A} I_{\beta}^{A} \mathcal{L}_{i\alpha}^{A}\mathcal{L}_{j\beta}^{A} \tag{2}$$

where $\mathcal{L}_{i\alpha}^{A} = 0.1$ is an occupation variable. In the Pink model the acyl chains in each monolayer are assumed to lie on a triangular lattice and each chain can be in 1 of 10 conformational states, $\alpha = 1, \ldots, 10$. The lipid bilayer is considered as being composed of two non-interacting monolayers. The model does therefore not directly account for possible effects due to chain interdigitation. Each acyl-chain conformational state is described by an internal conformational energy, E_{α}^{A}, a degeneracy, D_{α}^{A}, and a cross-sectional area A_{α}^{A} which is inversely related to the acyl-chain length, d_{α}^{A}, by the constant volume condition. The values of these single-chain properties for di-acyl saturated phosphatidylcholine bilayers have previously been determined by Pink et al. [21]. Π is an interfacial lateral pressure having a numerical value of 30 dyne/cm. The 10 states of the Pink model may be grouped in two sets, one consisting of nine conformationally ordered acyl-chain states (termed 'gel' states below) and one conformationally disordered acyl-chain state (termed the 'fluid' state below). An acyl chain interacts via van der Waals interactions of strength J_A with six nearest-neighbour acyl chains. This interaction is modulated by shape-dependent nematic order parameters, I_{α}^{A}. The values of the interaction strengths J_A, which we have derived by simple scaling from the previously determined value for $DC_{16}PC$ [25], are as follows, $J_A = 0.5232$, 0.618, 0.815, $0.915 \cdot 10^{-13}$ erg for DC_nPC with $n = 12$, 14, 18, 20, respectively.

The interaction between different lipid species is described by the Hamiltonian

$$\mathcal{H}^{AB} = \frac{-J_{AB}}{2}\sum_{i,j}\sum_{\alpha,\beta}\left(I_{\alpha}^{A} I_{\beta}^{B}\mathcal{L}_{i\alpha}^{A}\mathcal{L}_{j\beta}^{B} + I_{\alpha}^{B} I_{\beta}^{A}\mathcal{L}_{i\alpha}^{B}\mathcal{L}_{j\beta}^{A}\right)$$
$$+ \frac{\gamma}{2}\sum_{i,j}\sum_{\alpha,\beta}\left(\left|d_{i\alpha}^{A} - d_{j\beta}^{B}\right|\mathcal{L}_{i\alpha}^{A}\mathcal{L}_{j\beta}^{B}\right.$$
$$\left. + \left|d_{i\alpha}^{B} - d_{j\beta}^{A}\right|\mathcal{L}_{i\alpha}^{B}\mathcal{L}_{j\beta}^{A}\right) \tag{3}$$

The first term in $\mathcal{H}^{AB}$ describes the direct van der Waals hydrophobic contact interaction between different acyl chains. The corresponding interaction constant is taken to be the geometric average $J_{AB} = \sqrt{J_A J_B}$. γ in the second term of Eqn. 3 represents the mismatch interaction and is assumed to be 'universal' in the sense that its value does not depend on the lipid species in question. It was previously shown via a two-component regular solution theory [16] that a wide range of binary lipid phase diagrams, using a mean-field (phenomenological) version of Eqn. 3, could be described in terms of such a single universal parameter, once the chain-length characteristics were isolated in the chain-length variable d_{α}. We show below that a similar universal description is applicable to the full microscopic interaction model of Eqns. 1–3 when it is solved within a considerably more reliable calculational scheme than mean-field theory, i.e., by computer-simulation techniques as described below.

Calculational techniques

Monte Carlo computer-simulation techniques [25] offer a numerically exact way of deriving the thermodynamic properties of the molecular interaction model in Eqns. 1–3 using the principles of statistical mechanics. The particular virtue of computer simulations is that they ensure that the density- and the compositional fluctuations are accurately accounted for, and that the full entropy of mixing is automatically included in the description. Moreover, the simulations operate on the microscopic variables, and hence reveal the organization of the membrane system on all length scales up to the size of the system studied. In this way simulation techniques are unique in being able to determine local structure in lipid mixtures.

From the statistics generated in the computer simulations we have calculated the specific heat, $C_p(x_B, T)$, as a function of temperature for different compositions x_B with $1 = x_A + x_B$. From the features found in the specific heat it is possible to derive the form of phase diagrams for binary mixtures. Since conventional Monte Carlo simulations only allow us to determine derivatives of the free energy, such as the specific heat and not the free energy itself [25], we stress that our calculated phase diagrams are only approximate. In this sense the simulation approach suffers from the same shortcomings as many of the experimental determinations of the phase diagram. There is no experimental technique available which operates directly on the level of the free energy. It is, however, possible to employ more advanced numerical techniques than those used here which allow that part of the free energy to be determined that controls the relative stability of the different phases. These techniques, which use the fin-size scaling theory, were recently used to study the nature of the gel-fluid transition in pure lipid bilayers [26,27] and have been extended to the study of phase equilibria in lipid-polypeptide systems [24]. We did not use these time-intensive simulation techniques for the present problem, since we do not require a very accurate determination of the phase diagram in order to study local lipid structure well inside the various regions of the phase diagram.

The conventional Monte Carlo simulations on the model of Eqns. 1–3 lead to a determination of a series of microconfigurations for the system which are characteristic of equilibrium at the thermodynamic conditions chosen. Thermal equilibrium of the model system is attained using single-site Glauber excitation for the acyl-chain degrees of freedom on each lipid species and Kawasaki two-site exchange dynamics to simulate the interdiffusion of the two species. We have studied the mixture in the canonical ensemble, i.e., for fixed temperature and composition which is the way in which experiments are carried out. The simulations were performed on large periodic arrays of lipid chains, typically 100×100, in order to assure that the results are characteristic for the thermodynamic limit.

III. Materials and Methods

The lipids dimyristoyl phosphatidylcholine ($DC_{14}PC$) and distearoyl phosphatidylcholine ($DC_{18}PC$) were obtained from Avanti Polar Lipids (Birmingham, AL, USA) and used without further purification. Lipid mixtures were prepared by dissolving the appropriately weighed amount of the two lipids in chloroform. The organic solvent was removed using a rotary evaporator and then lyophilized for at least 12 h. Dried lipid was dispersed in buffer (50 mM KCl) at 60°C to form multilamellar vesicles. The dispersion was frozen (−70°C) and thawed (60°C) at least 4 times.

Differential scanning calorimetry was performed using a high-sensitivity calorimeter of the heat-conduction type [28]. Upscans at a scanrate of 20 C°/h were performed using 0.75 ml of 20-mM samples. Appropriate baselines have been subtracted from the excess heat capacity curves. No correction has been made for the time response of the calorimeter.

IV. Theoretical results

Specific heat and phase equilibria

Figs. 1 and 2 give the computer-simulation data for the specific-heat function, $C_p(x,T)$, in the full composition range for the two mixtures $DC_{14}PC$–$DC_{18}PC$ and $DC_{12}PC$–$DC_{18}PC$. The coexistence region is clearly reflected in the features found for C_p. The approximate phase diagrams, also shown in Figs. 1 and 2, were derived from the specific heat. Both mixtures show strong non-ideal mixing behavior. While the $DC_{14}PC$–$DC_{18}PC$ mixture has only a broad gel-fluid coexistence region, the $DC_{12}PC$–$DC_{18}PC$ mixture displays peritectic behavior with a pronounced three-phase line and gel-gel coexistence. As described in Section V below, both of these phase diagrams are in good agreement with the experimental data. There is still some controversy regarding the phase diagram for the $DC_{14}PC$–$DC_{18}PC$ mixture which has also been predicted to

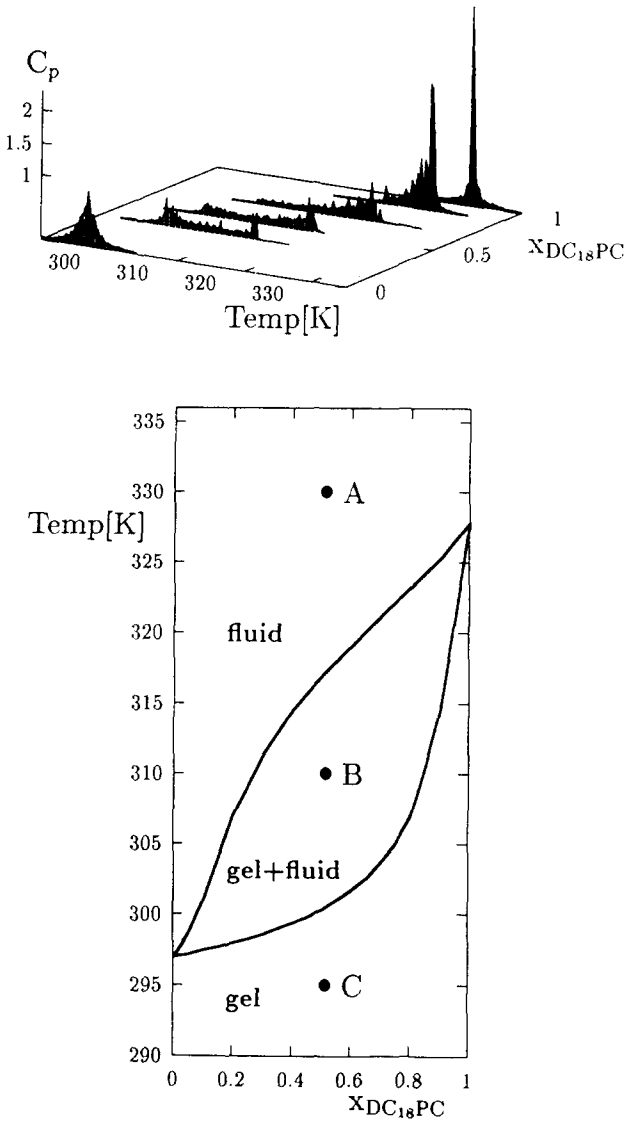

Fig. 1. $DC_{14}PC$–$DC_{18}PC$: Specific heat (top) and phase diagram (bottom) in the temperature-composition plane as obtained from the theoretical model. Membrane configurations at the three specific points A, B and C are shown in Fig. 3. The specific heat is in units of 10^{-13} erg/K.

display peritectic behavior [17,18]. We shall return to this controversy in another publication (Jørgensen, K. et al., unpublished data).

Phase separation and local lipid structure

Snapshots are shown in Fig. 3 of microscopic bilayer configurations typical of thermodynamic equilibrium at the three points, A, B, and C, indicated in the phase diagram in Fig. 1, i.e., typical of the fluid phase, the fluid-gel coexistence and the gel phase. The visual appearance of the phases clearly shows that frames A and C are one-phase regions while frame B displays macroscopic phase separation with a clear distinction between the two phases which are separated by a more or less well-defined interface. Nevertheless, even

though frame A and C contain one-phase regions of fluid and gel phase, respectively, these phases are clearly not uniform or random in structure: they exhibit considerable local structure, and chains of the same lipid species form large connected regions. Furthermore, the two phases making up the coexisting system in frame B each have their distinct local structure. The local structure both in the one-phase fluid region and in the two-phase gel-fluid coexistence region becomes more pronounced as the mixture becomes more non-ideal. This can be seen by comparing frames A and B of Fig. 3 for the $DC_{14}PC$–$DC_{18}PC$ mixture with frames A and B of Fig. 4 for the $DC_{12}PC$–$DC_{18}PC$ mixture. Later, we will examine the extreme case of a $DC_{12}PC$–$DC_{20}PC$ mixture (see Fig. 12). Frame C in Fig. 4 is an example of macroscopic gel-gel coexistence.

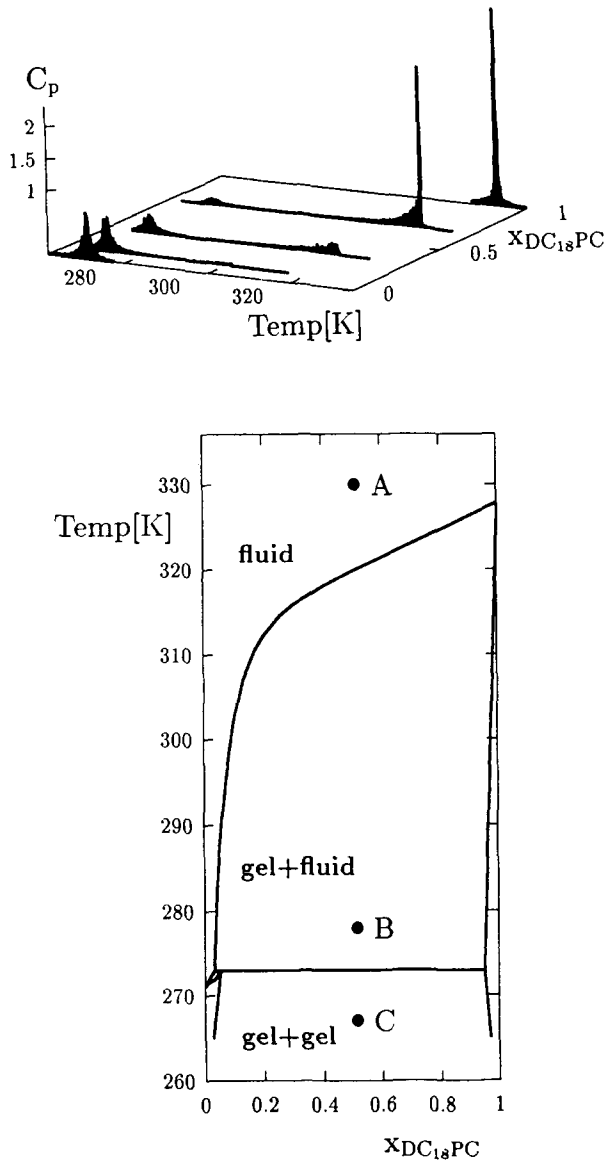

Fig. 2. $DC_{12}PC$–$DC_{18}PC$: Specific heat (top) and phase diagram (bottom) in the temperature-composition plane as obtained from the theoretical model. Membrane configurations at the three specific points A, B and C are shown in Fig. 4. The specific heat is in units of 10^{-13} erg/K.

Interfacial wetting and lipid enrichment

Frame B in Fig. 4 for the gel-fluid coexistence region of the $DC_{12}PC$–$DC_{18}PC$ mixture reveals an extremely interesting phenomenon of local interfacial ordering. The gel phase in the coexistence region is clearly wetted by a layer of gel-type acyl-chain configurations of the low-melting lipid $DC_{12}PC$. This layer, which extends over several acyl-chain diameters for the $DC_{12}PC$–$DC_{18}PC$ mixture, is not a static entity but is dynamically maintained. The interface of one type of gel lipids is enriched, in a statistical sense, by gel lipids of the other type. There is no binding or static annulus. Rather the wetting is induced by the hydrophobic matching condition inherent in Eqn. 3. The microscopic wetting effect, which may be considered a precursor effect for three-phase separation, is increased as the three-phase line is approached. At this line a real macroscopic wetting phenomenon is expected. Pronounced wetting of lipid domains in phase-separation regions is hence a distinct and organized form of dynamic local lipid structure.

A similar though less pronounced wetting effect is found in the gel-fluid coexistence region of the $DC_{14}PC$–$DC_{18}PC$ mixture (see, e.g., frame B of Fig. 3) where the gel-state lipids of the low-melting species together with fluid-state lipids of the high-melting lipid tend to accumulate at the interface of the gel phase.

The wetting of lipid-domain interfaces leads to a lowering of the interfacial tension similar to the effect discussed in the literature in relation to softening of pure lipid bilayers due to covering of gel-fluid interfaces by excited chain states [29,30]. The lowering of the interfacial tension implies a slowing down of the interfacial dynamics and an increase in the lifetime of the local structure.

Lipid-lipid correlation functions

A quantitative description of the degree of local structure in the lipid mixture is provided by the general static pair correlation function for species X and Y defined by

$$g_{\alpha\beta}(XY)(R) = \langle \mathcal{L}_{i\alpha}^{X}(R_i)\mathcal{L}_{j\beta}^{Y}(R_j)\rangle - \langle \mathcal{L}_{i\alpha}^{X}\rangle\langle \mathcal{L}_{j\beta}^{Y}\rangle \tag{4}$$

where $R = |R_i - R_j|$ is the distance in units of lattice spacings, X, Y = A, B, and α, β = g, f. For ease of calculation we only studied the simplest type of spatial autocorrelation function, i.e.,

$$g_{\alpha\alpha}(X)(R) = \langle \mathcal{L}_{i\alpha}^{X}(R_i)\mathcal{L}_{j\alpha}^{X}(R_j)\rangle - \langle \mathcal{L}_{i\alpha}^{X}\rangle^2. \tag{5}$$

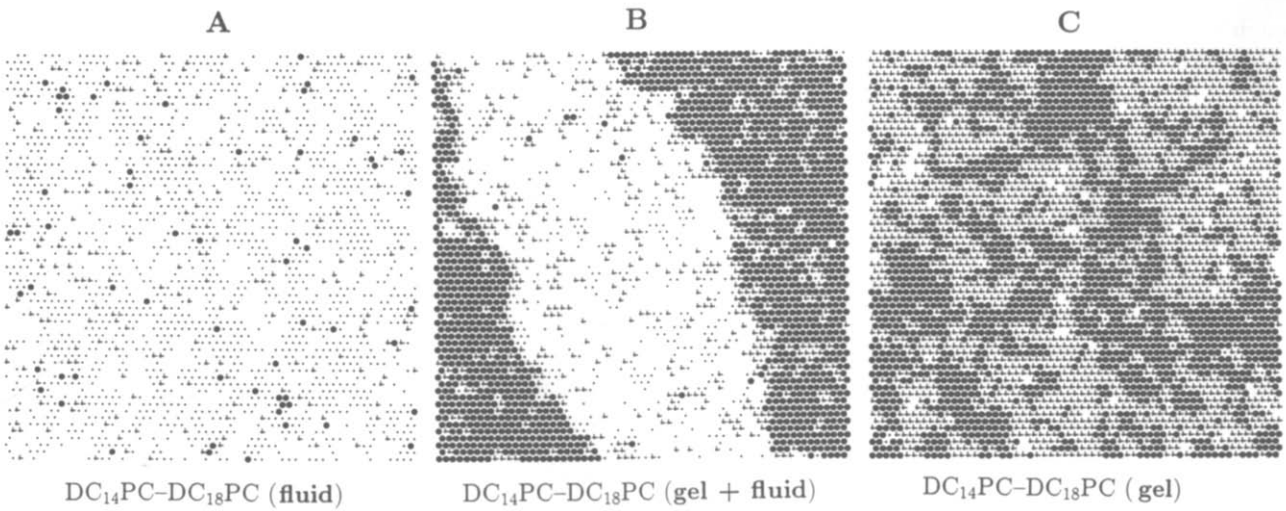

Fig. 3. $DC_{14}PC$–$DC_{18}PC$: Snapshots of microscopic membrane configurations with 60×60 acyl chains shown at points A ($T = 330$ K), B ($T = 310$ K) and C ($T = 295$ K) in the phase diagram as indicated in Fig. 1. The composition corresponds to $x_{DC_{18}PC} = 0.5$. The symbols for the chain states are as follows: gel-$DC_{14}PC$ (+), fluid-$DC_{14}PC$ (blank), gel-$DC_{18}PC$ (●), fluid-$DC_{18}PC$ (·).

The second term in Eqns. 4 and 5 corrects for the background correlation, i.e., the global concentration. Hence the correlation function is a measure of the correlation of both thermal and compositional fluctuations, thereby providing a complete description of short-range order effects and local structure.

Fig. 5 shows the correlation function $g_{ff}(DC_{18}PC)(R)$ in the fluid phase of the $DC_{14}PC$–$DC_{18}PC$ mixture at two different temperatures. It is seen that there is a substantial correlation in the position of like species and that the correlation length increases as the phase boundary is approached. The correlation function for the $DC_{14}PC$–$DC_{18}PC$ mixture in the full concentration range at $T = 330$ K is shown in Fig. 6. This function has two striking features. Firstly, the function is peaked around equimolar composition. This peak is controlled by the compositional fluctuations which we shall discuss later. Secondly, there is a another peak close to the axis of the high-melting lipid. At the temperature in question, we are above but close to the melting point of pure $DC_{18}PC$. Since we are dealing with the correlation function for the species $DC_{18}PC$, this second peak reflects the thermal density fluctuations at the gel-fluid transition of $DC_{18}PC$ [31]. If we now examine the same correlation function of the other species, $DC_{14}PC$, shown in Fig. 7, only the compositional fluctuation maximum remains, since $T = 330$ K is far above the transition temperature of pure $DC_{14}PC$ and its thermal density fluctuations are fully suppressed. It is, therefore, possible at $T = 330$ K to

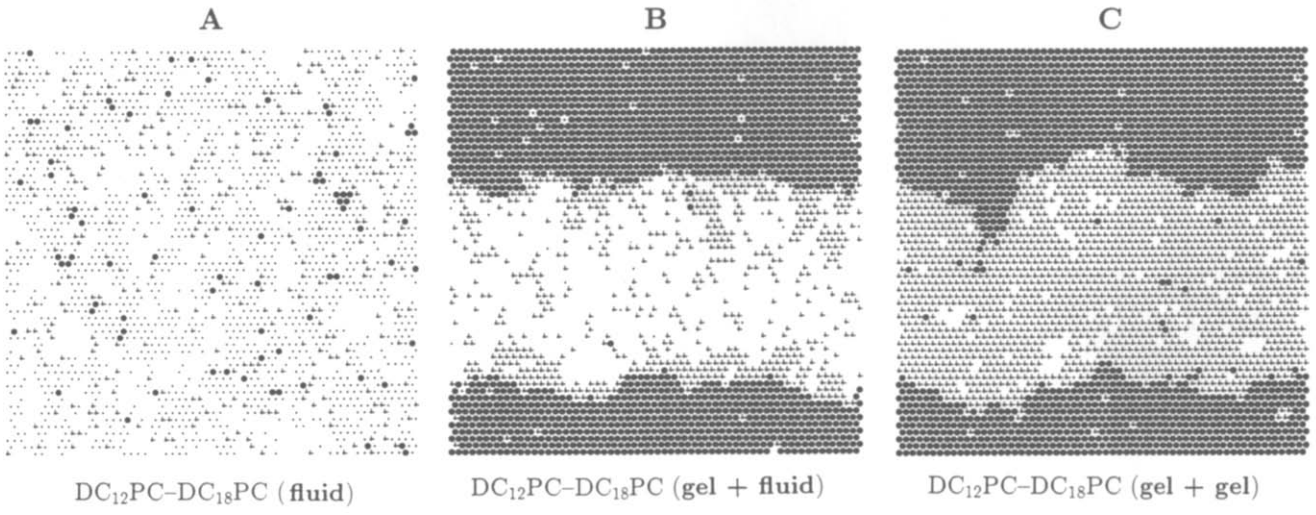

Fig. 4. $DC_{12}PC$–$DC_{18}PC$: Snapshots of microscopic membrane configurations with 60×60 acyl chains shown at points A ($T = 330$ K), B ($T = 278$ K) and C ($T = 265$ K) in the phase diagram as indicated in Fig. 2. The composition corresponds to $x_{DC_{18}PC} = 0.5$. The symbols for the chain states are as follows: gel-$DC_{12}PC$ (+), fluid-$DC_{12}PC$ (blank), gel-$DC_{18}PC$ (●), fluid-$DC_{18}PC$ (·).

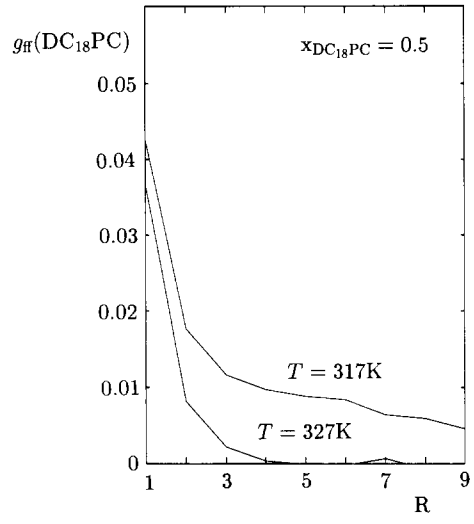

Fig. 5. $DC_{14}PC$–$DC_{18}PC$: Pair correlation function, $g_{ff}(DC_{18}PC)$ in Eqn. 5, at $x_{DC_{18}PC} = 0.5$ shown at two different temperatures in the fluid phase as a function of acyl-chain separation, R (in units of lattice spacings).

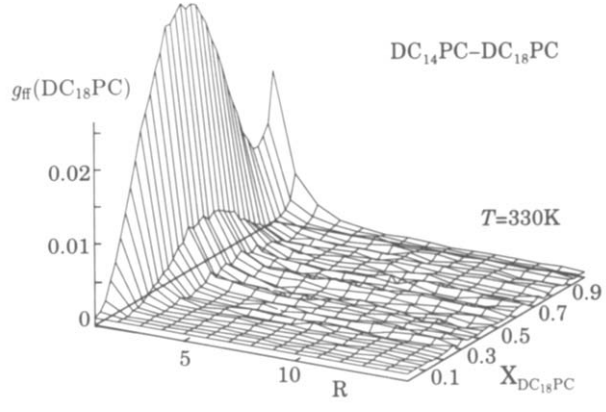

Fig. 6. $DC_{14}PC$–$DC_{18}PC$: Pair correlation function, $g_{ff}(DC_{18}PC)$ in Eqn. 5, as a function of acyl-chain separation, R (in units of lattice spacings), at $T = 330$ K shown in the full composition range.

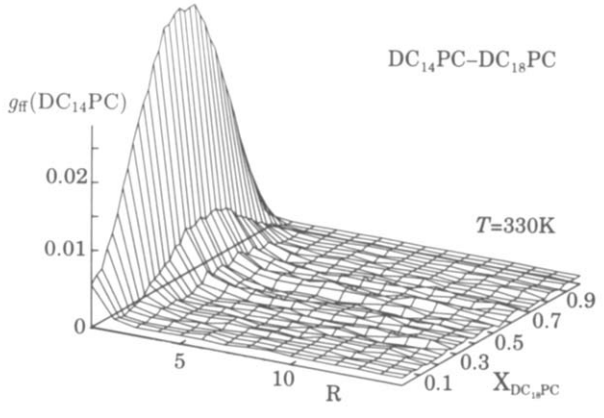

Fig. 7. $DC_{14}PC$–$DC_{18}PC$: Pair correlation function, $g_{ff}(DC_{14}PC)$ in Eqn. 5, as a function of acyl-chain separation, R (in units of lattice spacings), at $T = 330$ K shown in the full composition range.

focus on the density fluctuations alone by studying $g_{gg}(DC_{18}PC)(R)$ shown in Fig. 8. This figure shows that the correlation between the gel-state lipids of $DC_{18}PC$ increases as the concentration of $DC_{18}PC$ becomes higher and attains its maximum value for a bilayer composed of pure $DC_{18}PC$. Due to the high temperature in question, most of the gel-state lipids have melted and the remaining gel-states of the acyl chains no longer reflect the compositional fluctuations but rather the density fluctuations near the transition point of the high-melting lipid.

A visual impression of the local structure due to density fluctuations near the pure $DC_{18}PC$ melting point is given in Fig. 9 which shows a snapshot of a microscopic membrane configuration at $T = 330$ K and $x_{DC_{18}PC} = 0.97$. The density fluctuations clearly manifest themselves in the formation of gel clusters inside the fluid phase.

The correlation functions in the case of the $DC_{12}PC$–$DC_{18}PC$ as displayed in Figs. 10 and 11 show the same effects as for the $DC_{14}PC$–$DC_{18}PC$ mixture. The correlation length is, however, significantly larger.

An extreme case: the $DC_{12}PC$–$DC_{20}PC$ mixture

The effects of local lipid structure illustrated above via the correlation function can be studied under extreme conditions in the case of the $DC_{12}PC$–$DC_{20}PC$ mixture where the mismatch amounts to as much as 8 carbon atoms. The fluid phase shows a strong tendency for clustering of like lipids in a way which resembles microphase separation, cf., Fig. 12. The thermodynamic one-phase fluid region is highly structured. The correlation function $g_{ff}(DC_{20}PC)(R)$ in Fig. 13 shows a very long-range coherence due to the compositional fluctuations. The peak due to the density fluctuations near the pure $DC_{20}PC$ melting point is also visible in Fig. 13.

V. Comparison with experiments

We first make the observation that the phase diagrams shown in Figs. 1 and 2 for the $DC_{14}PC$–$DC_{18}PC$ and $DC_{12}PC$–$DC_{18}PC$ mixtures are in close quantitative agreement with experimental data (see Ref. 16 for a compilation of the available experimental data, as well as the recent experimental phase diagrams in Ref. 32). No phase diagram is at present available for the $DC_{12}PC$–$DC_{20}PC$ mixture. However, a detailed comparison between experimental and theoretical phase diagrams will be provided in a subsequent publication (Jørgensen, K., et al., unpublished data) for the full series of binary mixtures of the type considered here. It suffices to note that the model provides a good description of the experimental phase diagrams considered in the present paper.

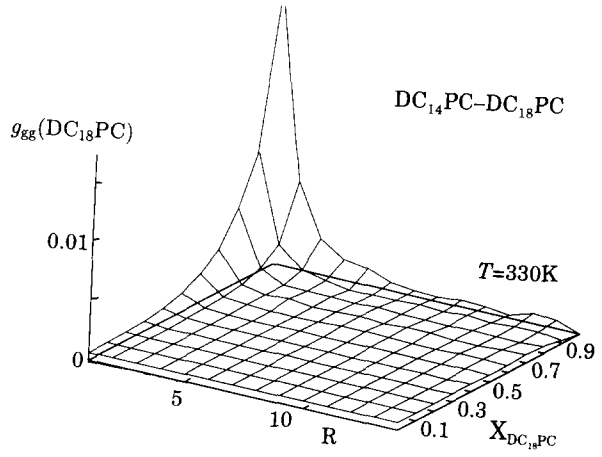

Fig. 8. $DC_{14}PC-DC_{18}PC$: Pair correlation function, $g_{gg}(DC_{18}PC)$ in Eqn. 5, as a function of chain separation, R (in units of lattice spacings), at $T = 330$ K shown in the full composition range.

Secondly, we compare in Fig. 14 the calculated specific-heat scan of Fig. 1 at $x_{DC_{18}PC} = 0.5$ with that obtained from our diffential-scanning calorimetry experiments. The quantitative agreement between theory and experiment is very satisfactory. Not only is the overall shape of the scans very similar, but indications of pronounced specific-heat wings below the solidus and above the liquidus lines are also present in both sets of data, signalling strong membrane fluctuations [20].

Finally, we note that compositional fluctuations are manifested in the structure factor of small-angle neutron scattering of lipid bilayer mixtures [17,18]. Data for the $DC_{14}PC-DC_{18}PC$ mixture have been interpreted [17,18] in terms of a critical demixing phenomonon assuming that an incipient critical gel-gel upper critical point is hidden in the gel-fluid coexistence region. This interpretation implies the existence

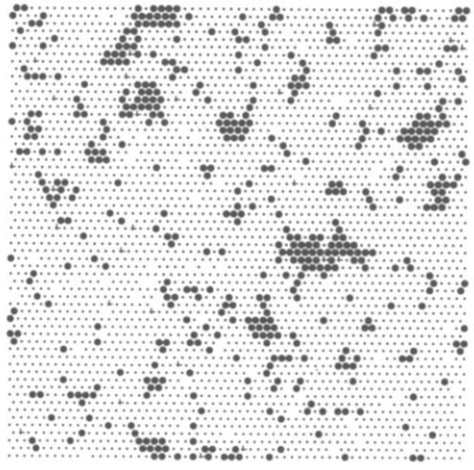

Fig. 9. $DC_{14}PC-DC_{18}PC$: Snapshot of a microscopic membrane configuration with 60×60 acyl chains shown at a temperature, $T = 330$ K and a composition, $x_{DC_{18}PC} = 0.97$, in the fluid phase close to the melting point of pure $DC_{18}PC$. The symbols used are explained in Fig. 3.

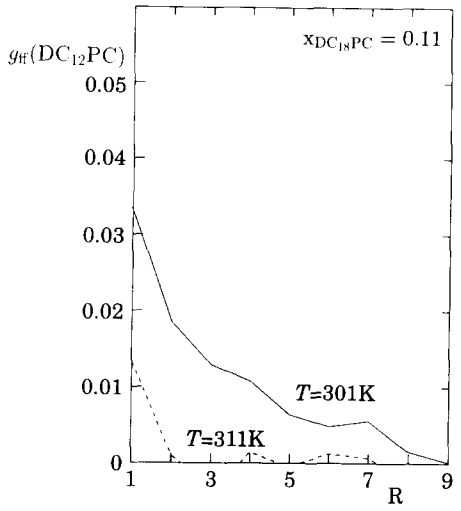

Fig. 10. $DC_{12}PC-DC_{18}PC$: Pair correlation function, $g_{ff}(DC_{12}PC)$ in Eqn. 5, at $x_{DC_{18}PC} = 0.5$ shown at two different temperatures in the fluid phase as a function of acyl-chain separation, R (in units of lattice spacings).

of peritectic behavior for the $DC_{14}PC-DC_{18}PC$ mixture and the presence of a three-phase line. Some experimental evidence in favor of the existence of a gel-gel coexistence region in this mixture has been presented, but the true phase behavior still remains an unresolved problem. Whatever the details of the phase diagram at lower temperatures, it is observed experimentally that the fluid phase of the $DC_{14}PC-DC_{18}PC$ mixture sustains large compositional fluctuations, especially near equimolar compositions, as found in the present model study. The experimental values quoted for the correlation length ξ are as large as 300 Å, which is somewhat larger than those obtained from the microscopic model of the mixture.

VI. Conclusions

We have presented results of model simulations, as well as experimental calorimetric data for two-compo-

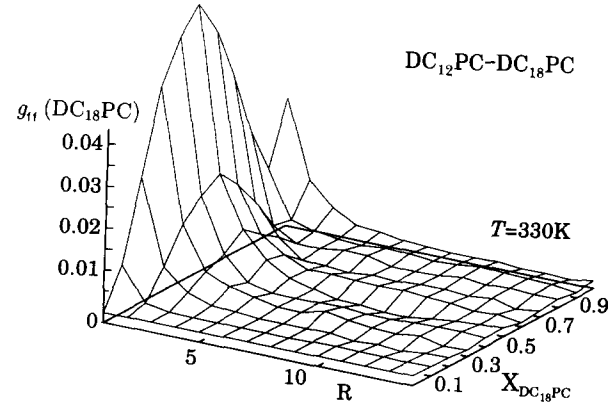

Fig. 11. $DC_{12}PC-DC_{18}PC$: Pair correlation function, $g_{ff}(DC_{18}PC)$ in Eqn. 5, as a function of acyl-chain separation, R (in units of lattice spacings), at $T = 330$ K shown in the full composition range.

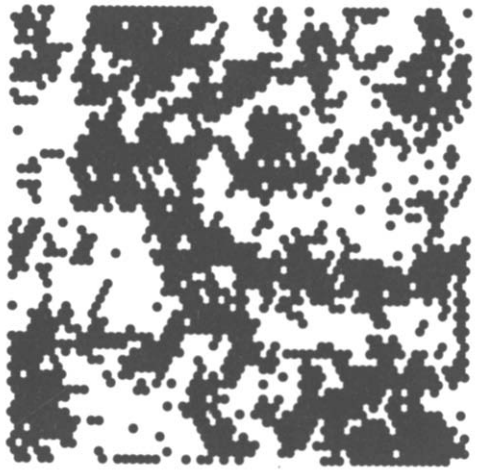

Fig. 12. $DC_{12}PC$–$DC_{20}PC$: Snapshot of a microscopic membrane configuration with 60×60 acyl chains shown at a temperature, $T = 338$ K and a composition, $x_{DC_{20}PC} = 0.5$, in the fluid phase. The symbols for the fluid chain states are as follows: fluid-$DC_{12}PC$ (blank) and fluid-$DC_{20}PC$ (•).

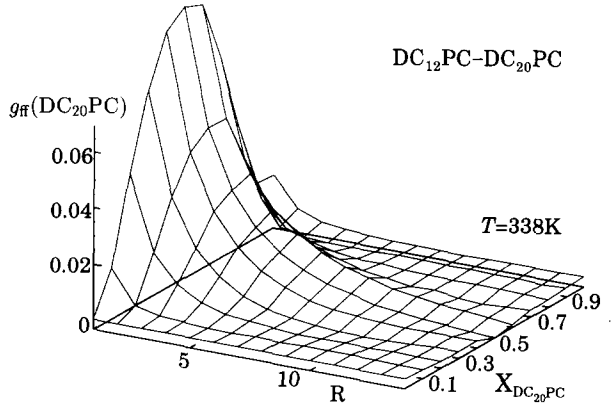

Fig. 13. $DC_{12}PC$–$DC_{20}PC$: Pair correlation function, $g_{ff}(DC_{20}PC)$ in Eqn. 5, as a function of acyl-chain separation, R (in units of lattice spacings), at $T = 338$ K shown in the full composition range.

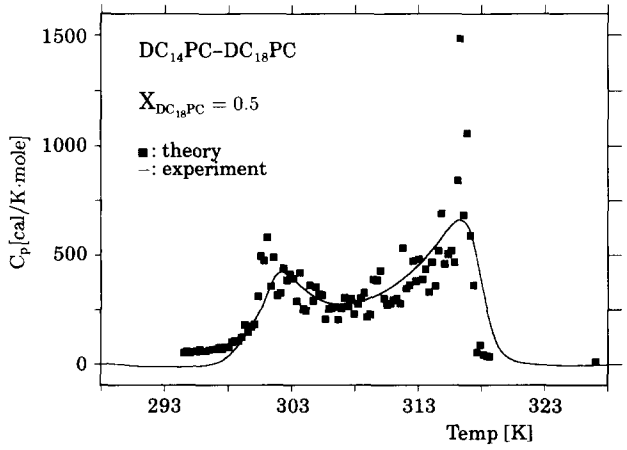

Fig. 14. $DC_{14}PC$–$DC_{18}PC$: Comparison between a theoretical (■), cf., Fig. 1 and an experimental (–) specific-heat scan at $x_{DC_{18}PC} = 0.5$. The experimental data is obtained at a scan rate of 20 C°/h.

nent phospholipid membranes of saturated phospholipids with different acyl-chain lengths. Our results show that the non-ideal mixing properties of the two lipids have a pronounced influence on the heterogeneous membrane behavior and the associated differentiated lateral organization of the membrane components. In the phase-separated regions an enrichment of the phase boundaries by one of the lipid species has been found, leading to a decrease of the interfacial tension between coexisting phases.

In particular we studied the fluid thermodynamic one-phase region and found that the phospholipids have a distinct non-random distribution manifested as a dynamic local lateral structure consisting of correlated lipids. The correlation length of these fluid structures is much smaller than the equivalent length scale characterizing the domains in the gel-fluid phase coexistence region [7,8,32]. The local structure becomes more pronounced as the degree of non-ideal mixing increases. Furthermore, percolation-like fluid structures develop for large mismatches between the hydrophobic acyl-chain lengths as seen in Fig. 12. The local structure also depends on the distance from the phase boundaries and it is most pronounced near equimolar concentrations, as was also found in earlier theoretical studies on phenomenological models of binary lipid mixtures [33–35]. The results presented here were derived for di-acyl PC mixtures but the effect of local structure in the fluid phase is expected to be quite general for two-component systems and should occur in any kind of binary lipid mixture, for example in mixtures where the non-ideality is induced by different polar head groups or by different degrees of unsaturation in the acyl chains of the two species. In particular, the occurrence of critical mixing in two-component lipid membranes is likely to be a widespread phenomenon. Similarly, local lipid structure should persist in mixtures of more than two lipid species.

Our results for local lipid ordering and structure in fluid lipid membranes may well be important for clarifying the possible functional role of different lipids in membranes and the selectivity in lipid-protein interactions. Specifically, it will be interesting to refine our model to allow for the more specific lipid-lipid interactions which are responsible for the regular distribution of lipids found in pyrene-PC/$DC_{14}PC$ binary mixtures [5,36].

It would clearly be worthwhile to expand the perspective of this paper to lipid-protein systems where there is considerable evidence that dynamic membrane heterogeneity and differentiated lateral membrane organization couple to enzymatic activity in both one- and two-component lipid membranes [13,14,20,37]. Another interesting consideration concerns the intricate action of drugs such as general and local anaesthetics on membrane functions which can be related to the

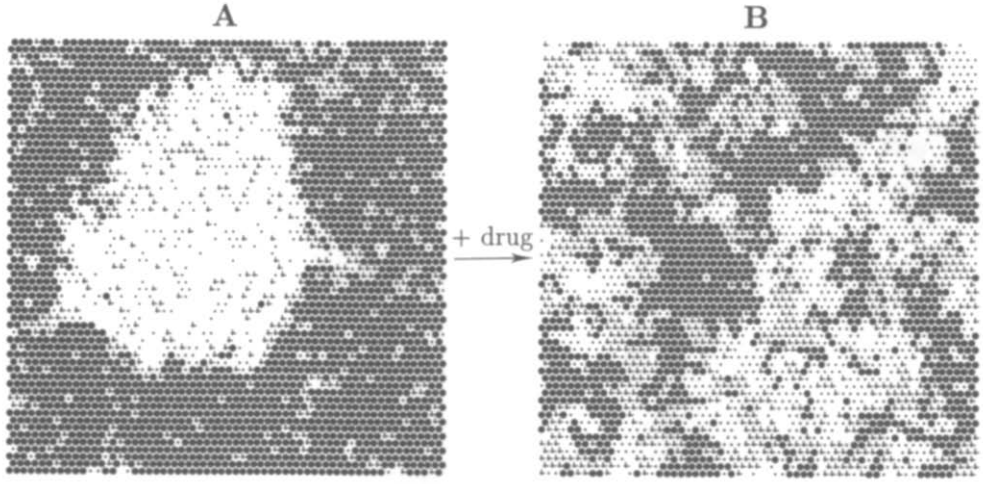

Fig. 15. $DC_{14}PC$–$DC_{18}PC$: The effect of adding a drug (like halothane or cocaine derivatives) on the bilayer structure in the gel-fluid coexistence region at $x_{DC_{18}PC} = 0.7$ and $T = 314$ K. The symbols are explained in Fig. 3.

physical effects of the drug on the global and local lipid structure [38–40]. It has been shown [41] that addition of general anaesthetics like methoxyfluorane to a two-component bilayer displaying phase separation might have a dramatic influence on the membrane structure. As a final consideration we briefly discuss an example of such a phenomenon in the case of the $DC_{14}PC$–$DC_{18}PC$ mixture to which a water-soluble drug has been added. The lipid-drug interactions and the lipid-water partitioning of the drug are modelled using a formalism which we have recently developed [38,39]. The particular drug considered here is that of a generic type such as halothane or a cocaine derivative which have similar effects on the thermodynamic properties of lipid bilayers. The drug molecules are assumed to intercalate interstitially in the closely packed molecular array of the lipid bilayer. Fig. 15 shows microconfigurations of the $DC_{14}PC$–$DC_{18}PC$ mixture in the gel-fluid coexistence region before and after the drug is added. The presence of the drug is seen to have a drastic effect on the lipid structure: the gel-fluid interfaces become quite ramified and the global structure of the systems resembles that of an isotropic system, although a substantial local lipid structure remains. It is as though the drug acts as an emulsifier in destroying the global phase structure. Further investigation of this problem is in progress.

Acknowledgements

This work was supported by the Jenny Vissing Fond (K.J.), the Carlsberg Foundation (M.M.S.), the Danish Natural Science Research Council under grant no. 11-0065-1, the NSERC of Canada and le FCAR du Quebec under a centre and a team grant.

References

1 Kinnunen, P.K.J. and Laggner, P. (1991) Chem. Phys. Lipids 57, 109–408.
2 Bloom, M., Evans, E. and Mouritsen, O.G. (1991) Q. Rev. Biophys. 24, 293–397.
3 Cevc, G. and D. March. (1987) Phospholipid Bilayers. Physical Principles and Models. Wiley, New York.
4 Sackmann, E. (1984) in Biological Membranes, Vol. 5 (Chapman, D., ed.), pp. 105–142, Academic Press, London.
5 Kinnunen, P.K.J. (1991) Chem. Phys. Lipids 57, 375–399.
6 Tate, M.W., Eikenberry, E.F., Turner, D.C., Shyamsunder, E. and Gruner, S.M. (1991) Chem. Phys. Lipids 57, 147–164.
7 Vaz, W.L.C., Melo, E.C.C. and Thompson, T.E. (1989) Biophys. J. 56, 869–876.
8 Vaz, W.L.C., Melo, E.C.C. and Thompson, T.E. (1989) Biophys. J. 58, 273–275.
9 Almeida, P.F.F., Vaz, W.C.C. and Thompson, T.E. (1992) Biochemistry 31, 7198–7210.
10 Sankaram, M.B., Marsh, D. and Thompson, T.E. (1992) Biophys. J. 63, 340–349.
11 Tocanne, J.F. Dupou-Cézanne, L., Lopez, A. and Tournier, J.F. (1989) FEBS Lett. 257, 10–16.
12 Melo, E.C.C., Lourtie, I.M., Sankaram, M.B., Thompson, T.E. and Vaz, W.L.C. (1992) Biophys. J. 63, 1506–1512.
13 Thompson, T.E., Sankaram, M.B. and Biltonen, R.L. (1992) Comments Mol. Cell. Biophys. 8, 1–15.
14 Mouritsen, O.G. and Jørgensen, K. (1991) Bioessays 14, 129–136.
15 Mouritsen, O.G. and Biltonen, R.L. (1993) in Protein–Lipid Interactions, New Comprehensive Biochemistry (Watts, A., ed.), pp. 1–39, Elsevier, Amsterdam.
16 Ipsen, J.H. and Mouritsen, O.G. (1988) Biochim. Biophys. Acta 944, 121–134.
17 Knoll, W., Ibel, K. and Sackmann, E. (1981) Biochemistry 20, 6379–6383.
18 Knoll, W., Schmidt, G. and Sackmann, E. (1983) J. Chem. Phys. 79, 3439–3442.
19 Mabrey, S. and Sturtevant, J.M. (1976) Proc. Natl. Acad. Sci. USA 73, 3862–3866.
20 Biltonen, R.L. (1990) J. Chem. Thermodyn. 22, 1–19.
21 Pink, D.A., Green, T.J. and Chapman, D. (1980) Biochemistry 19, 349–356.

22 Mouritsen, O.G. and Sperotto, M.M. (1993) in Thermodynamics of Surface Cell Receptors (Jackson, M., ed.), pp. 127–181, CRC Press, Boca Raton.
23 Mouritsen, O.G. and Bloom, M. (1993) Annu. Rev. Biophys. Biomol. Struct. 22, 147–171.
24 Zhang, Z., Sperotto, M.M., Zuckermann, M.J. and Mouritsen, O.G. (1993) Biochim. Biophys. Acta 1147, 154–160.
25 Mouritsen, O.G. (1990) in Molecular Description of Biological Membrane Components by Computer Aided Conformational Analysis, Vol. 1 (Brasseur, R., ed.), pp. 3–83, CRC Press, Boca Raton.
26 Zhang, Z., Laradji, M., Guo, H., Mouritsen, O.G. and Zuckermann, M.J. (1992) Phys. Rev. A 45, 7560–7567.
27 Zhang, Z., Zuckermann, M.J. and Mouritsen, O.G. (1992) Phys. Rev. A 46, 6707–6713.
28 Suurkuusk, J., Lentz, B.R., Barenholz, Y., Biltonen, R.L. and Thompson, T.E. (1976) Biochemistry 15, 1393–1401.
29 Mouritsen, O.G. and Zuckermann, M.J. (1985) Eur. Biophys. J. 12, 75–86.
30 Mouritsen, O.G. (1991) Chem. Phys. Lipids 57, 178–194.
31 Ipsen, J.H., Jørgensen, K. and Mouritsen, O.G. (1990) Biophys. J. 58, 1099–1107.
32 Sankaram, M.B. and Thompson, T.E. (1992) Biochemistry 31, 8258–8268.
33 Freire, E. and Snyder, B. (1980) Biochim. Biophys. Acta 600, 643–654.
34 Freire, E. and Snyder, B. (1980) Biochemistry 19, 88–94.
35 Jan, N., Lookman, T. and Pink, D.A. (1984) Biochemistry 23, 3227–3231.
36 Tang, D. and Chong, L.-G. (1992) Biophys. J. 63, 903–910.
37 Goormaghtigh, E., Van Campenhoud, M. and Ruysschart, J.M. (1981) Biochem. Biophys. Res. Commun. 101, 1410–1418.
38 Jørgensen, K., Ipsen, J.H., Mouritsen, O.G., Bennett, D. and Zuckermann, M.J. (1991) Biochim. Biophys. Acta 1067, 241–253.
39 Jørgensen, K., Ipsen, J.H., Mouritsen, O.G. and Zuckermann, M.J. (1993) Chem. Phys. Lipids, in press.
40 Van Osdol, W., Ye, Q., Johnson, M.L. and Biltonen, R.L. (1992) Biophys. J. 63, 1011–1017.
41 Galla, H.J. and Trudell, J.R. (1981) Mol. Pharmacol. 19, 432–437.